RESEARCH ARTICLE

Society For Biomaterials   WILEY

Initial bone tissue reactions of hydroxyapatite/collagen–(3-glycidoxypropyl)trimethoxysilane injectable bone paste

Taira Sato[1,2] | Yuki Shirosaki[3] | Sho Oshima[1,4] | Kanji Tsuru[5] | Yoshihisa Koyama[1] | Mamoru Aizawa[2] | Masanori Kikuchi[1] 🟢

[1]Bioceramics Group, Biomaterials Field, Research Center for Macromolecules and Biomaterials, National Institute for Materials Science, Tsukuba, Ibaraki, Japan

[2]Department of Applied Chemistry, Graduate School of Science and Technology, Meiji University, Kawasaki, Kanagawa, Japan

[3]Department of Materials Science, Faculty of Engineering, Kyushu Institute of Technology, Kitakyushu, Fukuoka, Japan

[4]Department of Mechanical Engineering, Graduate School of Science and Engineering, Ibaraki University, Mito, Ibaraki, Japan

[5]Section of Bioengineering, Department of Dental Engineering, Fukuoka Dental College, Sawara, Fukuoka, Japan

Correspondence
Masanori Kikuchi, Bioceramics Group, Biomaterials Field, Research Center for Macromolecules and Biomaterials, National Institute for Materials Science, 1-1 Namiki, Tsukuba, Ibaraki 305-0044, Japan.
Email: KIKUCHI.Masanori@nims.go.jp

Present addresses
Taira Sato, Section of Biomaterials, Department of Dental Engineering, Fukuoka Dental College, 2-15-1 Tamura, Sawara 814-0193, Fukuoka, Japan; and Sho Oshima, General Affairs Department, Japan Carbon Frontier Organization, 3F Daiwa Nishi-shimbashi Building, 3-2-1 Nishi-shimbashi, Minato-ku 105-0003, Tokyo, Japan.

Abstract

We have previously reported that a novel bioresorbable self-setting injectable bone paste composed of hydroxyapatite/collagen bone-like nanocomposite (HAp/Col) and (3-glycidoxypropyl)trimethoxysilane (GPTMS) was successfully prepared and was replaced with new bone within 3 months of implantation in defects created in porcine tibia. In this study, the HAp/Col-GPTMS paste was implanted into bone defects in rat tibiae to investigate the initial kinetics and bone tissue response. Even though more than 35% of GPTMS molecules should be eluted rapidly from directly injected pastes according to previously reported cell culture tests, in this study, energy-dispersive X-ray spectrometry did not detect Si (GPTMS) deposition in tissues surrounding the paste at 1 day postimplantation. Further, no abnormal inflammatory responses were observed in the surrounding tissues over the test period for both directly injected and prehardened pastes. Companying these observations with the results of the previous animal test (in which the paste was fully resorbed and was substituted with new bone), the eluted GPTMS resolved in no harm in vivo from the initial to final (completely resorbed) stages. Material resorption rates calculated from X-ray microcomputed tomography (μ-CT) images decreased with increasing in GPTMS concentration. Histological observations indicated that tartrate-resistant acid phosphatase (TRAP) active cells, (assumed to be osteoclasts), exist on the periphery of pastes. This result suggested that the paste was resorbed by osteoclasts in the same way as the HAp/Col. Since a good correlation was observed between TRAP active areas in histological sections and material resorption rate calculated from μ-CT, the TRAP activity coverage ratio offers the possibility to estimate the osteoclastic resorption ratio of materials, which are replaced with bone via bone remodeling process.

KEYWORDS
(3-glycidoxypropyl)trimethoxysilane, bioresorbability evaluation, bone tissue reaction, hydroxyapatite/collagen, injectable bone paste

1 | INTRODUCTION

Bioresorbable and injectable bone fillers have been the key factors in growing the market over the past two decades, because they are strongly associated with reducing patient burden including surgical operation time, recovery time through minimally invasive surgery, risk of fracture, and so on. Therefore, the combination of these properties could induce further reductions in patients burden and further accelerate of market growth. Konishi et al. reported the preparation of novel chelate-setting α- and β-tricalcium phosphate (α- and β-TCP) pastes with bioresorbablity and self-setting ability utilizing inositol-6-phosphate (IP-6) as a chelating agent.[1] However, the mechanisms underpinning the resorption of β-TCP are unclear and there is a lack of evidence of osteoclastic resorption in clinical application where large quantities of β-TCP were implanted.[2–5] Furthermore, even though IP-6 is used as a food additive, there have been few studies on its use for implantation and metabolism in vivo.

Recently, we have reported the production of paste based on hydroxyapatite/collagen bone-like nanocomposite (HAp/Col)[6,7] powder utilizing (3-glycidoxypropyl)trimethoxysilane (GPTMS) aqueous solution as a liquid phase, and preliminary animal tests demonstrated excellent bone substitution in 3 months in porcine tibia without any systemic or local symptoms.[8] However, the cell culture test in the previous work also showed that increasing the amount of the GPTMS in HAp/Col-GPTMS paste inhibited cell proliferation in a static cell culture environment. This result suggests potential risks for cell and tissue reactions of the GPTMS leaching from the HAp/Col-GPTMS paste, which cannot be eliminated from the viewpoint of the following hardening mechanism. The hardening mechanism of the HAp/Col-GPTMS paste is divided into two parts, one is a bonding reaction between the amino group on collagen and epoxy group of GPTMS.[9,10] The other is a siloxane network formation by via a silane coupling agent, that is, self-condensation of silanol groups of silane coupling agent formed by its hydrolysis.[11–13] Our previous study indicated these hardening reactions of the HAp/Col-GPTMS pastes proceeded rapidly within 30 min; thus, GPTMS molecules are considered to be leached from the paste during hardening at the initial stage of implantation, as observed in the previous cell culture tests.

In the present study, influences of initially leached GPTMS and the substitution process of the HAp/Col-GPTMS with new bone were investigated through initial tissue reaction of the paste in rat tibia. Inflammatory reactions of surrounding tissues and dispersion of GPTMS of the HAp/Col-GPTMS paste from immediately after implantation to 7 days were investigated by direct injection (DI) of the paste into a hole created on tibia of SD-rats. The resorption process of the paste was studied in detail by implantation of the prehardened (PH) HAp/Col-GPTMS paste, to control shape of implant, into a hole created on tibia of SD-rats up to 4 weeks.

2 | MATERIALS AND METHODS

2.1 | Materials

The powder phase of the HAp/Col-GPTMS paste was prepared according to the previous report.[8]

The prepared HAp/Col powder was sterilized with ethanol aqueous solution at 70% in volume. The liquid phase of the paste was 1.0 or 10% in volume of GPTMS (TCI, Tokyo, Japan) aqueous solution, and these were hydrolyzed for 1 h prior to mixing with the powder phase. The liquid phases were sterilized with a filter (Milipore Millex-HV PVDF membrane filter 0.45 μm, Merck, Darmstadt, Germany). Pastes were prepared by mixing the HAp/Col powder and the GPTMS aqueous solution at the ratio of 1.00 g/cm^3, which was the optimal ratio determined in the previous report in terms of the compressive strength and the degradation-properties measured by a Japanese Industrial Standard JIS T 0330–4 "Bioceramics-Part 4: Physicochemical characterization of calcium phosphate bone paste." The pastes prepared with the respective concentrations of GPTMS solution are abbreviated as G[GPTMS concentration]-paste, for example, the HAp/Col paste prepared with 1.0% GPTMS solution is denoted as "G1.0-paste."

Hematoxylin–eosin (HE) staining was performed with Mayer's hematoxylin solution (Wako Pure Chemicals Inc., Japan) and 0.5% eosin Y, ethanol solution (Wako Pure Chemicals Inc., Japan), and a tartrate-resistant acid phosphatase (TRAP) stain was performed using TRAP/ALP stain kit (Wako Pure Chemicals Inc., Japan).

The test animals used in this study were 8-week-old male SD-rats.

2.2 | Dispersibility of the GPTMS and initial inflammatory reactions in vivo

This animal test was approved by the Institutional Animal Care and Use Committee of National Institute for Materials Science (Permission number: 49-2016-2) and which was carried out according to the committee's guidelines. The DI G1.0- and G10-pastes prepared on site were immediately and randomly implanted into holes in the tibial bone of 2.0 mm in diameter prepared by using a surgical drill under physiological saline injection. The implantation periods were 1, 2, 3, and 7 days. Following implantation, the rats were sacrificed to harvest the implant sites with the surrounding tissues. The harvested pastes and surrounding tissues were fixed with 70% ethanol and were observed with the naked-eye and an X-ray microcomputed tomograph (μ-CT; inspeXio SMX-90CT, shimadzu, Tokyo, Japan). The specimens were then dehydrated in a graded series of ethanol, cleared with Histo-clear® (National Diagnostics, Atlanta, USA), embedded in poly(methyl methacrylate) (PMMA) resin (OsteoResin Embedding Kit, FUJIFILM Wako Pure Chemical Industries, Ltd., Osaka, Japan), sliced with low speed saw and were carbon-coated for observation using an energy-dispersive X-ray spectrometer (EDS; Model JED-2300, JEOL Co. Ltd. Tokyo, Japan) at an acceleration voltage of 20 kV for elemental analyses and mappings.

2.3 | Bioresorbability and bone tissue responses

This animal test was approved by the Institutional Animal Care and Use Committee of National Institute for Materials Science (Permission

number: 49-2016-3) and which was carried out according to the committee's guidelines.

The paste for implantation was prepared as follows: the mold for prehardening was prepared by punching out a 2-mm thick silicone

determined by average of the measurement of the five test pieces immersed in phosphate buffered saline for each test period. The material reduction ratios were then calculated by the following formula.

$$\text{Material reduction ratio}(\%) = \frac{\text{Standard volume}(\text{mm}^3) - \text{Sample volume}(\text{mm}^3)}{\text{Standard volume}(\text{mm}^3)} \times 100 \tag{1}$$

rubber sheet using a 2 mm punch. The G1.0- and G10 pastes for the test were filled in the mold and PH in an incubator at 37°C for 72 h. The positive control (PC) was a HAp/Col dense body with the same shape as the paste sample, which was dehydrothermally cross linked at 140°C for 12 h and was sterilized with ethylene oxide gas. The samples were randomly implanted into tibial bone holes at 2.0 mm in diameter prepared using a surgical drill under physiological saline injection. The implantation periods were 1, 2, and 4 weeks. Numbers of specimen for the experimental and the PC groups were 4 and 3 for each period, respectively. Calcein (Dojindo Laboratories, Kumamoto, Japan) was injected to rats to label mineralizing bone at 2 weeks after implantation. After each implantation period, rats were sacrificed, and the samples and surrounding tissues were harvested and observed with the naked-eye. Immediately after harvest, the samples for HE

After the μ-CT analysis, the specimens for the HE and TRAP staining were decalcified by soaking for 2-week in 10% ethylenediaminetetraacetic acid disodium salts solution, which was exchanged every day. The specimen was then dehydrated via serial dilution of ethanol from 50% to 100% followed by immersion in Histo-Clear®, and was embedded in molten paraffin by the conventional method. Tissue blocks were stained by HE or TRAP after being sectioned at 5 μm with a microtome (SM2000R, Leica, Wetzlar, Germany). The stained histological sections were observed with an optical microscope. Lengths of the sample perimeter and that contacted with the TRAP activity marker of histological observation images were measured with ImageJ (National Institute of Health, ver. 1.46, for Mac). The TRAP activity coverage ratios were calculated from a following formula.

$$\text{TRAP coverage}(\%) = \frac{\text{Partial perimeter lenghth contacted with TRAP marker}(-)}{\text{Full perimeter length of the residual sample}(-)} \times 100 \tag{2}$$

and TRAP stained sections were fixed with 10% formalin neutral buffer solution, and those for Villanueva bone stained sections were fixed with 70% ethanol. Thereafter, the fixed specimens were analyzed with the μ-CT of which the spatial resolution was approximately 0.019 mm/pixel at an X-ray tube voltage of 90 kV and current of 110 μA. The residual volume of the material was calculated by analyzing the μ-CT images with the VGStudio MAX2.1 software (Volume Graphics GmbH, Heidelberg, Germany). In detail, the pastes portions in the μ-CT images were extracted as a region of interest, and its volumes were measured. The sample volume was the average residual volume of the specimens at each test period. Since the HAp/Col-GPTMS pastes and HAp/Col dense body swell when exposed to the body fluid, standard volume of the specimens at each test period was

The specimens for Villanueva bone stain after fixation were immersed in the Villanueva bone stain solution (Wako Pure Chemicals Inc., Japan) for 2 weeks and were embedded in PMMA resin. Subsequently, histological section with a thickness of about 10 μm was prepared using a diamond disc microtome (SP1600, Leica, Wetzlar, Germany) and were observed with a fluorescence microscope (DP70, Olympus, Tokyo, Japan).

2.4 | Statistical analysis

The results are shown as the mean ± standard deviation. Statistical significance was evaluated by the student's t test and was set at $p < .05$.
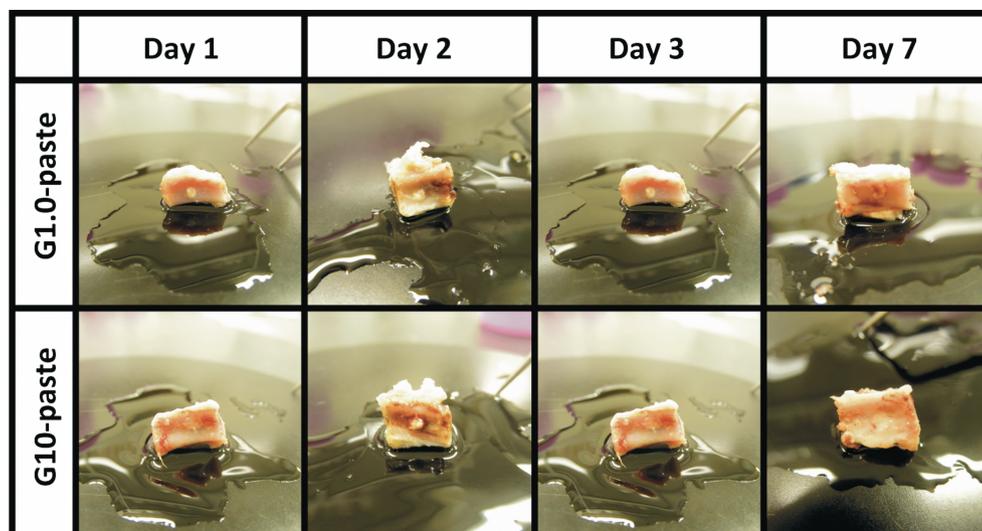
FIGURE 1 The naked eye images of the pastes with bone tissues within 1 week implantation.
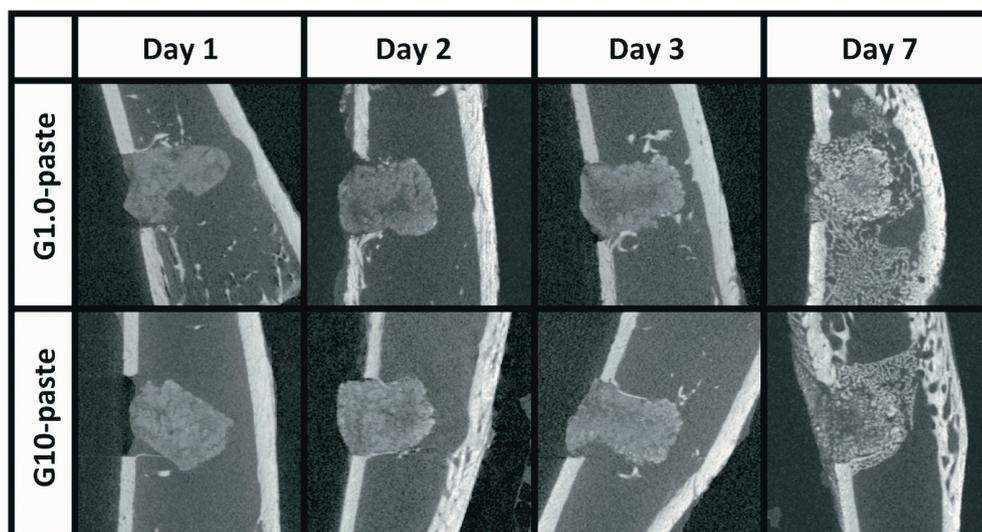

FIGURE 2 The microcomputed tomography (μ-CT) cross section images of the pastes with bone tissues within 1 week implantation.

3 | RESULTS

3.1 | GPTMS dispersibility and initial inflammatory reactions

No irregular inflammatory signs were observed during the implantation period and the harvested tissues as shown in Figure 1. Figure 2 summarizes the μ-CT images for each experimental period. Both the DI and PH pastes showed no degradation after implantation. No significant changes in volume and density of the pastes were observed from 1 to 3 days in both G1.0- and G10-pastes. The pastes at the 7 days after implantation swelled, and pores were formed by infiltration of bone marrow fluid; therefore, boundary phase between the paste and surrounding bone marrows was not clearly distinguished. From the EDS elemental analysis, no obvious Si peak was detected by point analysis even in the G10-paste region at first day, in which the highest Si signal should be detected (Figure 3). Elemental mapping analyses demonstrated that no high concentration regions of Si

were found in the paste and its surrounding tissues for all specimens.

3.2 | Bioresorbability and bone tissue responses

The PH pastes were a pseudo-cylindrical (hourglass) shape with a 2.0 mm in diameter and 2.0 mm in height, contrarily PC was cylindrical shape with a 2.0 mm in diameter and 2.0 mm in height. Figure 4A shows the μ-CT images of the specimens with surrounding tissues. The volume of the G1.0-pastes decreased with increasing in the implantation period, and the paste were covered with bone-like tissues. However, the shape of the G10-paste was almost unchanged during test period. The X-ray opacity of the PC reduced over time and volume of the PC could not be measured due to unclear boundaries between the PC and surrounding tissues. The material reduction ratios are illustrated in Figure 4B. The material reduction ratios of the paste increased with increasing in the implantation period.

FIGURE 3 The energy-dispersive X-ray spectrum of the G10-paste part of first day.
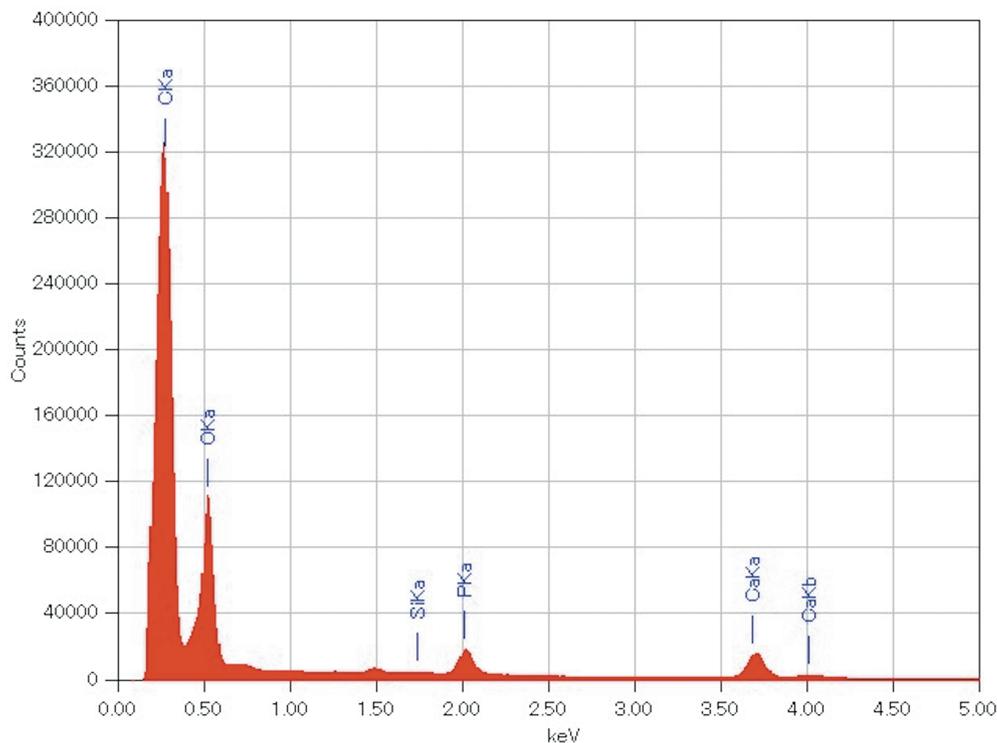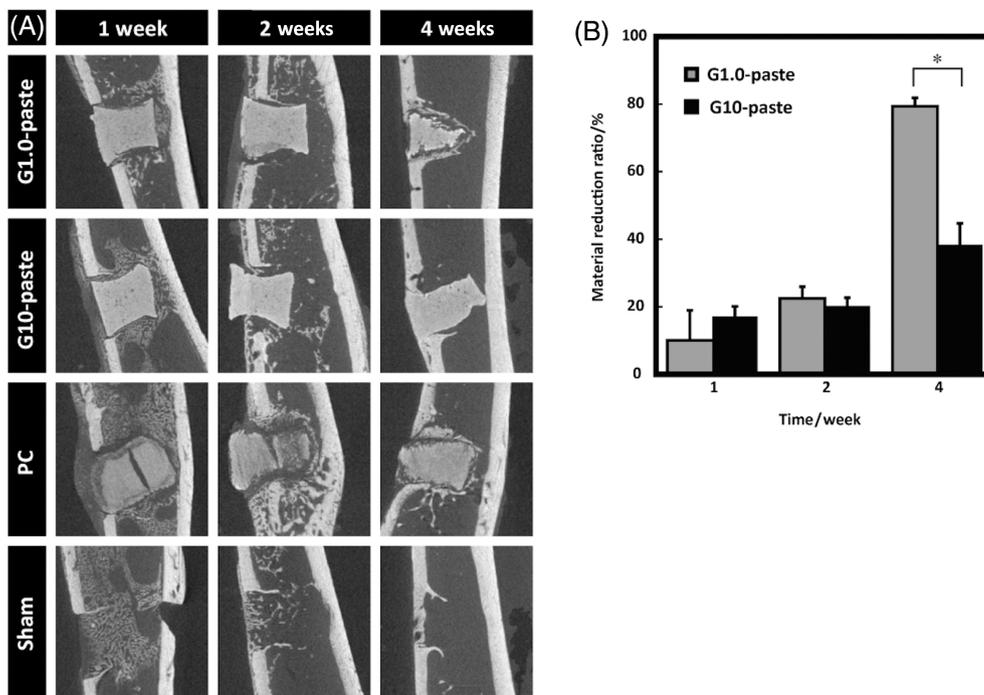

FIGURE 4 The microcomputed tomography (µ-CT) cross section images of the pastes with bone tissues within 4 weeks implantation (A) and material reduction ratio measured by image analysis (B). * $p < .05$. PC, positive control.

Low magnification HE stained histological sections shown in Figure 5A exhibited osteogenic responses but no irregular inflammatory cells recruitment occurred around any of the implanted materials over the entire test period. Figure 5B, high-magnification images of each yellow-bordered square in Figure 5A, shows that deeply dyed cell-nuclei around the material appeared from the first week observation. Further, the cell penetrations into gaps of the materials were observed from the first week of the PC and from the fourth week of the G1.0-paste. Figure 6 demonstrates TRAP stained sections at low (A) and high (B) magnifications. The low magnification images, Figure 6A, suggest that no TRAP active cells appeared on all the sham controls during the test period; in contrast, TRAP active cells appeared on both G1.0- and G10-pastes from the first week as well as the PC, and expression ratios of TRAP active cells were periodically increased until the fourth week. Furthermore, high magnification images, Figure 6B, revealed direct contact of TRAP-positive cells to the
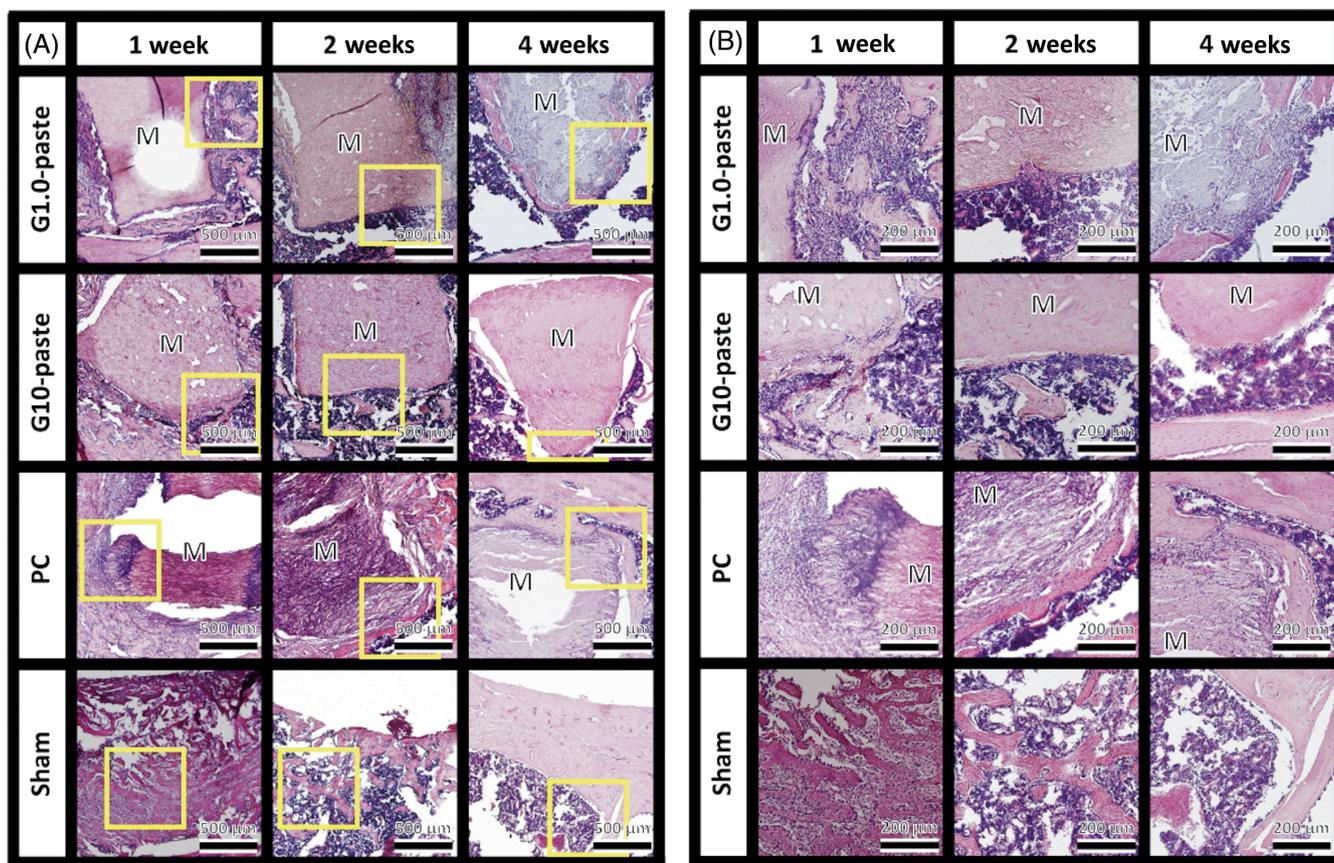
FIGURE 5 (A) Histological observation images of HE staining specimens. (B) Magnification of the area indicated by the yellow square in (A). "M"s indicate material portion. PC, positive control.

material. Figure 6C illustrates the TRAP coverage ratios. The TRAP coverage ratio of the G1.0-paste increased drastically with increasing in the implantation period. Although the G10-paste demonstrated higher TRAP coverage ratio than G1.0-paste at the first week, the TRAP coverage ratios of the G10-paste at the second and fourth weeks, approximately doubled from the first week, restrained to a half to one-third values than those of the G1.0-paste.

Figure 7A shows the fluorescence microscopy images of undecalcified sections with Villanueva bone stain. Red stained osteoid-like tissues were found at the drilling regions of sham site and the surroundings of all implanted materials at the first week and attenuated over time. At 4 weeks after implantation, the remaining G1.0-paste was covered with layers in the following order; cells, osteoid-like tissue, calcified bone, and calcein-labeled calcified bone as shown in Figure 7B. On the other hand, the G10-paste was directly covered with calcein-labeled calcified bone tissue without any other tissues between them (Figure 7C).

4 | DISCUSSION

As predicted from our previous results on cytocompatibility and preliminary animal tests,[8] no irregular inflammation signs were observed in the present animal studies as indicated in Figures 1 and 5.

The previous work reveals that approximately 35% of GPTMS in the pastes leached from the HAp/Col-GPTMS paste by 1 day immersion in cell culture medium.[3] Thus, the EDS analysis in this study was expected the detection of Si signal from the remaining GPTMS, approximately 65% of initial amount, in the pastes; because preliminary EDS analysis clearly detected Si signal from as-prepared G1.0-paste at P/L = 1.00 (data not shown). Contrary to expectation, no obvious Si signal was detected in all the implanted samples; therefore, the GPTMS released for all the paste samples after implantation was below the detection limit and far less than that of the G1.0-paste at P/L = 1.00 before implantation. In other words, body fluid circulation caused more GPTMS leaching than static in vitro conditions. Nevertheless, whole body and surrounding tissues showed no adverse effect, that is, leached GPTMS from the present pastes, 300 μg in maximum equivalent to 1000 μg/kg, was nontoxic at all for SD-rats. No significant degradation of the DI pastes, (in which amount of the GPTMS was far lower than the PH pastes), indicated that the HAp/-Col-GPTMS pastes were stable, which is important for use as a bone void filler material.

In Figure 4A, reducing X-ray opacity and gap formation of the PC could be caused by swelling of the PC that was also observed for ex vivo soaking in water. Due to the difference in preparation methods, swelling with gap formation was not observed in the pastes. The PC was prepared by squeezing out the water with a uniaxial-press followed
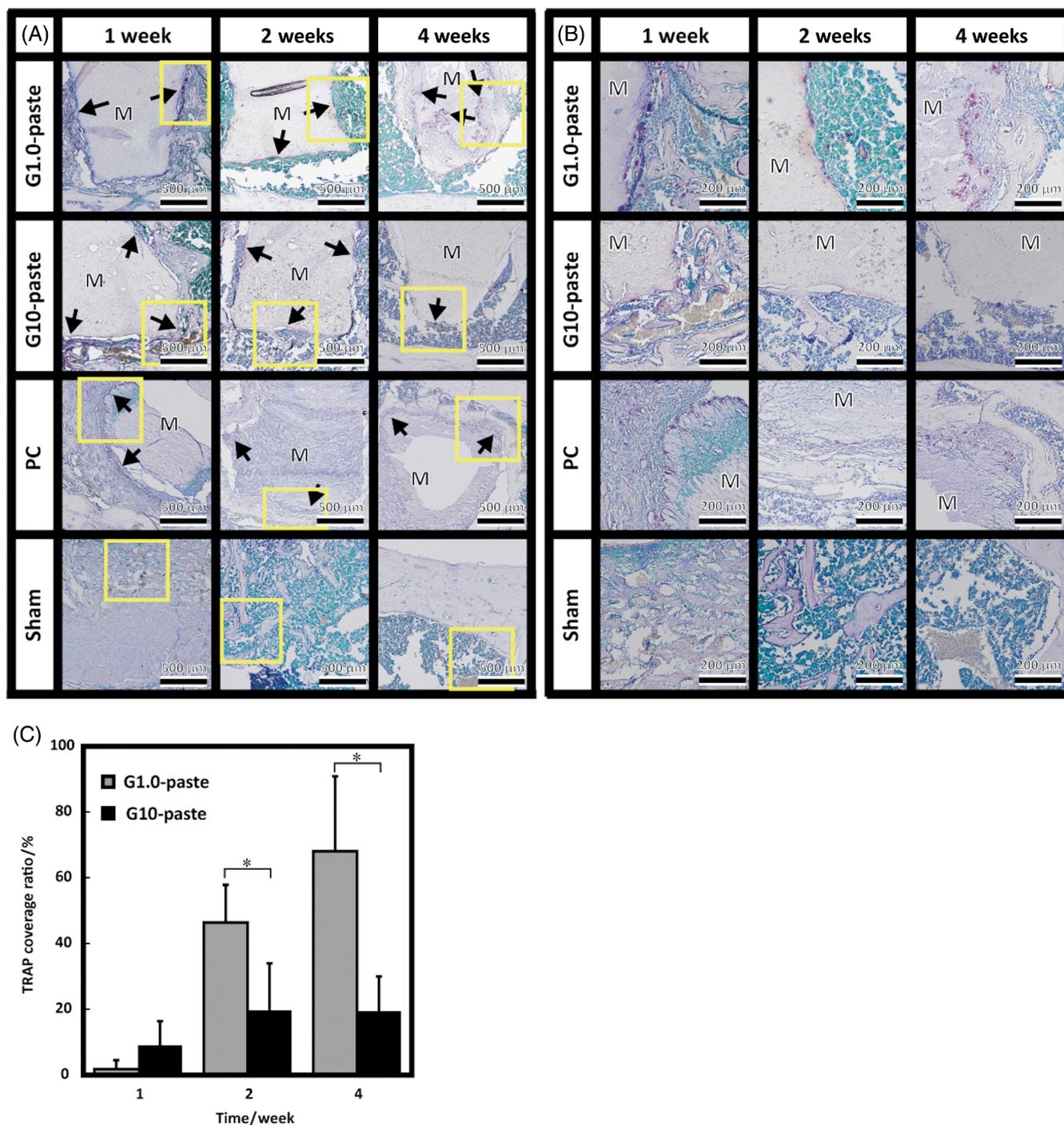
FIGURE 6 (A) Histological observation images of tartrate-resistant acid phosphatase (TRAP) staining specimens. Arrows indicate TRAP activity cells. (B) Magnification of the area indicated by the yellow square in (A). "M"s indicate material portion. (C) The TRAP activity coverage ratio calculated from image analysis. *$p < .05$. PC, positive control.

by freeze–drying and dehydrothermal cross-link of collagen in the HAp/Col; therefore, the PC had lamellar-like structure, from the stacking of the HAp/Col fibers. Accordingly, swelling of the HAp/Col fibers in the PC formed gaps by detaching of lamellar-like layers (or fibers) by breaking of weak parts of cross-links. Thus, cells penetrated only into the gap of PC at the first week as shown in Figure 5. In contrast, the

pastes were essentially a homogeneous hydrogel of HAp/Col powder and GPTMS; thus, they showed isotropic swelling and no gap formation. Furthermore, the preexisting water in the pastes, 60%–70% of the paste volume, and siloxane networks reduced swelling induced by infiltration of body fluids. The PH G10-paste, the paste with the highest hydrogel concentration, showed no swelling in the histological
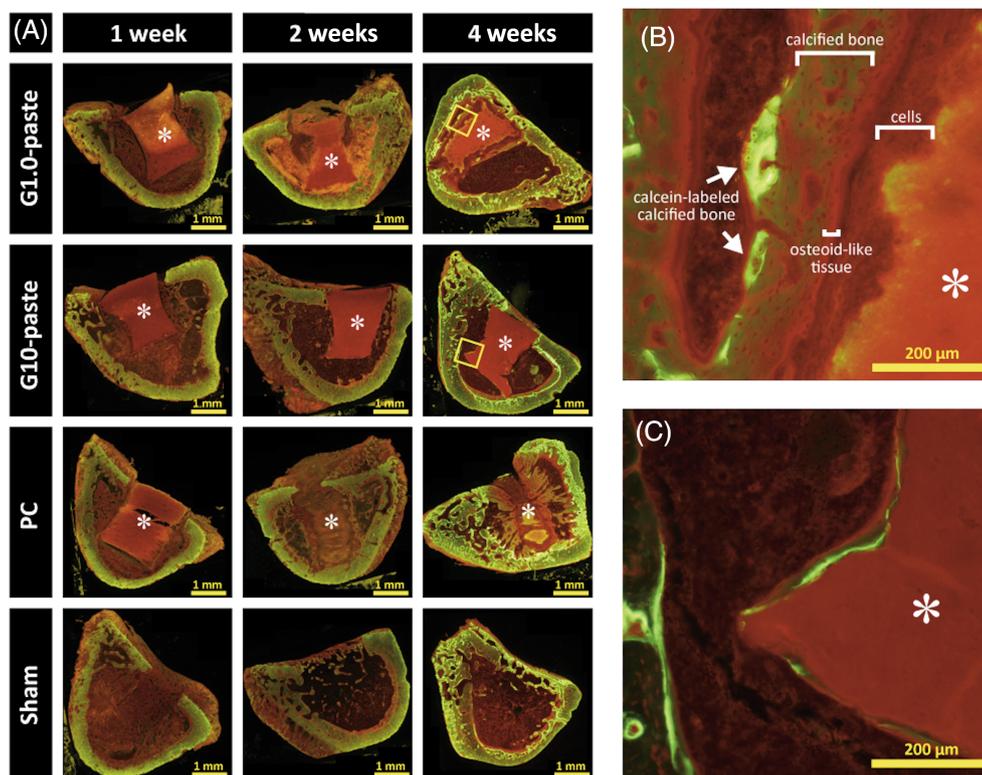
FIGURE 7 Histological observation images of Villanueva bone staining specimens (A). Magnification image of the G1.0-paste at 4 weeks after implantation (B). Magnification image of the G10-paste at 4 weeks after implantation (C). Stars indicate material portion. PC, positive control.
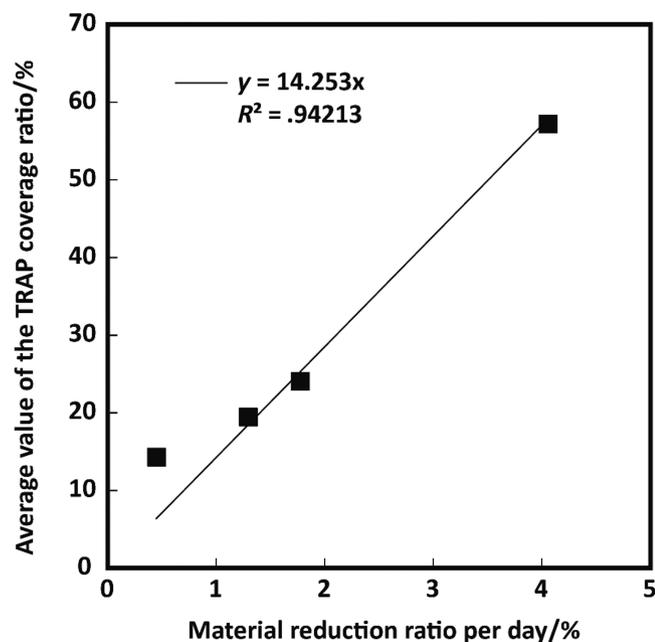

FIGURE 8 Relation of the material reduction ratio per day and average value of the tartrate-resistant acid phosphatase (TRAP) coverage ratio.

observation after 4 weeks. However, the DI pastes underwent swelling and absorption from day seven after implantation as observed with μ-CT images, because the DI paste formed less of a siloxane network structure than PH paste, due to significant leaching of GPTMS from the DI paste before hardening, that is, hydrogel formation.

The reverse relation between material reduction rates and GPTMS concentration illustrated in Figure 4B was explained by both collagen cross-link and siloxane network densities formed by GPTMS, that is, the higher densities of the collagen cross-link and the siloxane network, the lower resorption rate of the paste. Similar results have been reported that resorption rate of glutaraldehyde cross-linked HAp/Col dense body depended on the treatment concentration of glutaraldehyde.[14]

Body fluid is essentially supersaturated to HAp, and no significant dissolution of HAp is generally observed for sintered HAp and the HAp/Col (PC). Therefore, the reduction of the pastes in vivo is considered to be mainly caused by osteoclastic resorption, similarly to the PC. In fact, a lot of TRAP-positive multinucleated giant cells, osteoclasts, was adhered on the paste as observed in Figure 6. Furthermore, Figures 5, 6, and 7A demonstrated bone-like tissue formation at the surroundings of the resorbed paste. These bone-like tissues would attenuate following to the general repair process as revealed in the preliminary animal test in our previous work.[8] These results demonstrated that the HAp/Col-GPTMS pastes, as well as the PC, follow the required process for bioresorption of bone substitute materials proposed by Hannink et al.,[15] that is, new bone would be formed by osteoblasts following to the resorption of the paste by osteoclasts. In fact, even though the G10-pastes had the slowest resorption rates, the TRAP coverage ratio was maintained and the material reduction ratio increased from the second to fourth weeks. In addition, formation of calcein-labeled calcified bone was observed surrounding the G10-pastes and the results of the previous animal

test led to the conclusion that the G10-pastes would eventually be replaced with new bone within 3 months.

As described above, in order for bone substitute materials to be replaced by new bone, they should induce osteoclastic resorption beforehand bone formation; thus, estimation of their osteoclastic resorption from some factor(s) would be helpful to research the new bone substitute materials. For this reason, the validity of the average TRAP activity coverage ratio in this study as a factor for presumption of osteoclastic resorption was verified. The HAp/Col can be used to obtain exact osteoclastic resorption amounts, because the HAp/Col is not dissolved by body fluid; thus, the daily material reduction ratio can be applied for approximation of daily osteoclastic resorption ratio. As demonstrated in Figure 8, a relation between the daily material reduction ratio and TRAP activity coverage ratio showed linear approximation with $R^2 = .94213$; therefore, the TRAP activity coverage ratio offers the possibility to estimate the daily osteoclastic resorption ratio of bone substitute materials, at least for the HAp/Col-based bone void fillers. Further validations are, of course, necessary to apply the index to other bone substitute materials, because inorganic ions and proteins in the material composition and the solubility of the material would influence the material resorption rate.[16,17]

5 | CONCLUSION

Molecules of GPTMS in the DI pastes eluted rapidly from them and diffused with dissipation from surrounding tissues; however, no obvious adverse reactions, including severe inflammation, were detected. Further, both DI and PH pastes showed no obvious adverse reactions over the test period including osteoclastic resorption process; thus, the pastes were safe during substitution process with new bone. As previously reported, all the pastes were resorbed by osteoclasts followed by bone formation, probably by osteoblasts, at the lacunae, as the same as the HAp/Col dense and porous bodies. Considering these data with the previous pig experiment, which showed complete substitution of the paste with new bone, the HAp/Col pastes are good candidates for an excellent bone paste that is fully incorporated into the bone remodeling process. Further, the TRAP activity coverage ratio could be used to estimate of the daily osteoclastic resorption ratio of bone substitute materials, at least for the HAp/Col-based bone void fillers.

DATA AVAILABILITY STATEMENT
Research data are not shared.

ORCID
Masanori Kikuchi https://orcid.org/0000-0002-9451-8147

REFERENCES

1. Konishi T, Takahashi S, Zhuang Z, et al. Biodegradable β-tricalciumphosphate cement with anti-washout property based on chelatesettingmechanism of inositol phosphate. *J Mater Sci Mater Med*. 2013;24:1383-1394.
2. Ogose A, Kondo N, Umezu H, et al. Histological assessment in grafts of highly purified beta-tricalcium phosphate (OSferions®) in human bones. *Biomaterials*. 2006;27:1542-1549.
3. Sotome S, Ae K, Okawa A, et al. Efficacy and safety of porous hydroxyapatite/type 1 collagen composite implantation for bone regeneration: a randomized controlled study. *J Orthop Sci*. 2016;21:373-380.
4. Barralet J, Akao M, Aoki H, Aoki H. Dissolution of dense carbonate apatite subcutaneously implanted in Wister rats. *J Biomed Mater Res*. 2000;49:176-182.
5. Yuan H, Yang Z, Bruijn JD, de Groot K, Zhang X. Material-dependent bone induction by calcium phosphate ceramics: a 2.5-year study in dog. *Biomaterials*. 2001;22:2617-2623.
6. Kikuchi M, Itoh S, Ichinose S, Shinomiya K, Tanaka J. Self-organization mechanism in a bone-like hydroxyapatite/collagen nanocomposite synthesized in vitro and its biological reaction in vivo. *Biomaterials*. 2001;22:1705-1711.
7. Kikuchi M, Ikoma T, Itoh S, et al. Biomimetic synthesis of bone-like nanocomposites using the self-organization mechanism of hydroxyapatite and collagen. *Compos Sci Technol*. 2004;64:819-825.
8. Sato T, Shirosaki Y, Nagaya M, et al. Preparation of anti-decay self-setting pastes of hydroxyapatite/collagen utilizing (3-glycidoxypropyl) trimethoxysilane. *J Asian Ceramic Soc*. 2018;6:322-331.
9. Chen S, Chinnathambi S, Shi X, Osaka A, Zhu Y, Hanagata N. Fabrication of novel collagen-silica hybrid membranes with tailored biodegradation and strong cell contact guidance ability. *J Mater Chem*. 2012;22:21885-21892.
10. Ren L, Tsuru K, Hayakawa S, Osaka A. Novelapproach to fabricate porous gelatin-siloxane hybrids for bone tissue engineering. *Biomaterials*. 2002;23:4765-4773.
11. Labella R, Braden M, Deba S. Novel hydroxyapatitebased dental composites. *Biomaterials*. 1994;15(15):1197-1200.
12. Wang M, Bonfield W. Chemically coupled hydroxyapatite– polyethylene composites: structure and properties. *Biomaterials*. 2001;22(11):1311-1320.
13. Plueddemann EP. *Chemistry of Silane Coupling Agents*. Springer; 1991.
14. Kikuchi M, Matsumoto HN, Yamada T, Koyama Y, Takakuda K, Tanaka J. Glutaraldehyde cross-linked hydroxyapatite/collagen self-organized nanocomposites. *Biomaterials*. 2004;25:63-69.
15. Hannink G, Arts JC. Bioresorbability, porosity and mechanical strength of bone substitutes: what is optimal for bone regeneration? *Injury*. 2011;42:S22-S25.
16. Lakhkar NJ, Lee IH, Kim HW, Salih V, Wall IB, Knowles JC. Bone formation controlled by biologically relevant inorganic ions: role and controlled delivery from phosphate-based glasses. *Adv Drug Deliv Rev*. 2013;65:405-420.
17. Boyle WJ, Simonet WS, Lacey DL. Osteoclast differentiation and activation. *Nature*. 2003;423:337-342.